STRUCTURE OF MATTER
AND QUANTUM CHEMISTRY

Quantum-Chemical Modeling of Ethylene and Acetylene Adsorption on Gold Clusters

D. A. Pichugina, S. A. Nikolaev, D. F. Mukhametzyanova, and N. E. Kuz'menko

Faculty of Chemistry, Moscow State University, Moscow, Russia
e-mail: dashapi@mail.ru

Abstract—The interaction of ethylene and acetylene molecules with planar (2D) and nonplanar (3D) gold clusters Au_n ($n = 10, 12, 20$) was studied by the density functional theory (DFT) method. The coordination of hydrocarbons at the vertices, edges, and fragments of the Au_3 cluster was shown to form π, di-σ, and μ type complexes, respectively. The standard Gibbs energy and the C–C bond length of the hydrocarbon change during its adsorption in the series $\mu > $ di-$\sigma > \pi$ complexes. The highest selectivity in adsorption of acetylene relative to that of ethylene was achieved on Au_{12} (3D) and Au_{20} (2D) clusters.

Keywords: gold clusters, ethylene, acetylene, adsorption, quantum chemistry, density functional theory.

INTRODUCTION

Gold nanoparticles are active catalysts of the oxidation of CO, alkanes, and alcohols [1, 2]; hydrodechlorination of chloroaromatic compounds [3]; and allyl isomerization of alkenes [4]. Recently, gold-containing catalysts were found to be highly active in the hydrogenation of acetylene hydrocarbons into the corresponding alkenes [5, 6]. The technological significance of this process depends on the necessity of preliminary purification of the ethylene raw material from the acetylene impurity in the synthesis of high-quality polymers [7].

For selective hydrogenation of acetylene, the acetylene molecules should be bound to the active center of the catalyst more strongly than the ethylene molecules [8]. As is known, the tightness of substrate–catalyst surface binding is largely determined by the type of the adsorbed complex [8–10]. When interacting with transition metals, acetylene and ethylene can form π, di-σ, and μ type complexes [7–11]. The complexation involves the π electrons of the hydrocarbon and the electronic system of one metal atom for the π complex; the electronic systems of two carbon atoms and two metal atoms for the di-σ complex; and the electronic systems of two carbon atoms and three metal atoms for the μ complex.

The type of the resulting complex and the degree of activation of the hydrocarbon depend on the structural and electronic features of the cluster. The structurally nonrigid (dynamic) clusters are characterized by minor energy change during the hydrocarbon adsorption and facilitate the activation of the C–C bond [12, 13]. The formation of adsorbed complexes is accompanied by a redistribution of electron density in the carbon–metal system [11]. Consequently, the C–C

bond activation is strongly affected by the electronic structure of the cluster, in particular, the energy difference between the highest occupied molecular orbital and the lowest unoccupied molecular orbital [14].

Recently, theoretical approaches have started to be actively used for structure elucidation and studies of the adsorption properties of clusters [14–18]. It was predicted, using a quantum-chemical calculation, that the Au_{20} atomic cluster has a tetrahedral structure [18]. Later, this was confirmed experimentally using electron microscopy [16] (Fig. 1a). Density functional theory (DFT) calculations showed that the nickel atoms in the Au_xNi_y clusters bind carbon more weakly than in Ni_x [2]. On the basis of the results of these studies, Au–Ni catalysts were created which had high stability against deactivation in the vapor conversion of butane [2].

This communication presents the results of our quantum-chemical modeling of the effect of the structure of gold clusters on ethylene and acetylene adsorption. We considered planar (2D) clusters Au_{10}, Au_{12}, and Au_{20} (Fig. 2a–c), which were models of the structural units of small gold particles immobilized on the substrate surface [16, 19] and their three-dimensional (3D) isomers (Fig. 1d–f). The changes in the standard Gibbs energy during the formation of π, di-σ, and μ complexes of ethylene and acetylene with gold clusters were calculated. For most stable clusters, the selectivity in the adsorption of acetylene relative to that of ethylene was evaluated.

CALCULATION PROCEDURE

The geometry was optimized and the energies of the clusters and their hydrocarbon complexes were
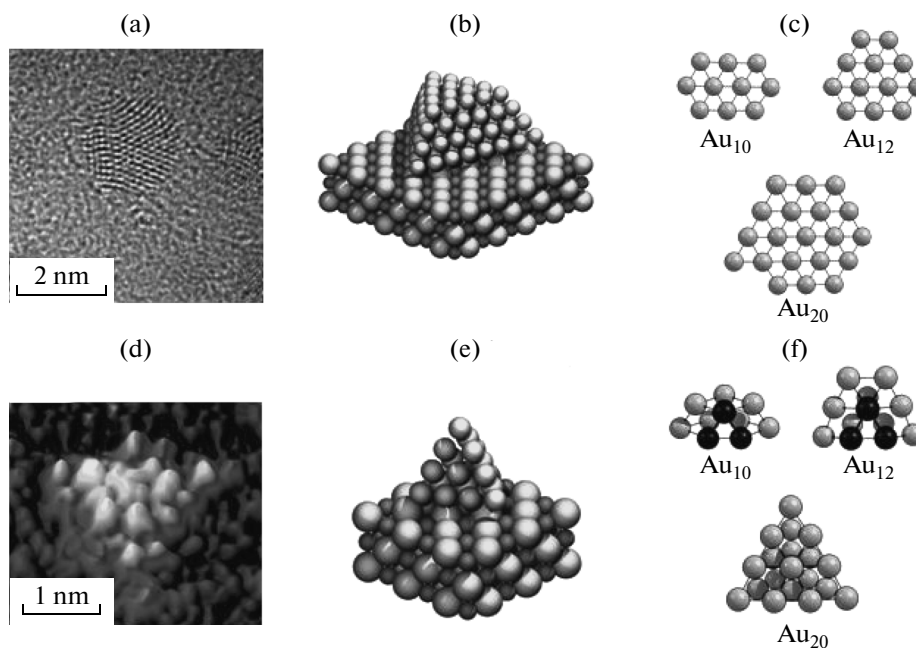
Fig. 1. (a, d) Micrographs of differently shaped gold particles immobilized on the substrate [16, 19]; (b, e) models of the surface of these systems; and (c, f) gold clusters studied in this work.
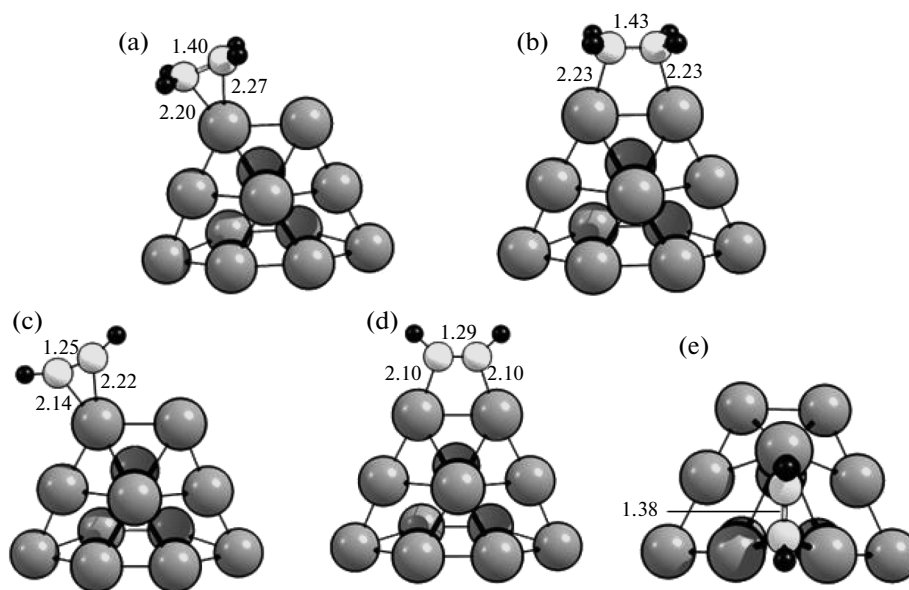
Fig. 2. Optimized structures of the complexes (a) π-$C_2H_4Au_{12}$, (b) di-σ-$C_2H_4Au_{12}$, (c) π-$C_2H_4Au_{12}$, (d) di-σ-$C_2H_2Au_{12}$, and (f) μ-$C_2H_2Au_{12}$. The key atomic distances are given in Å.

calculated by the DFT method using the PBE (Perdew−Burke−Ernzerhof) functional [20] in a scalar relativistic approximation [21]. The calculations were performed with the Priroda 06 program [22] using the basis functions Au $\{30s29p20d14f\}/[8s7p5d2f]$, H $\{6s2p\}/[2s1p]$, and C $\{10s7p3d\}/[3s2p1d]$. This approach was used earlier for calculating the structure and energies of gold clusters [10, 17, 23]. The Au_{10},

Au_{12}, and Au_{20} clusters were obtained by structure optimization based on the literature data [18, 24, 25]. For ethylene and acetylene, the π, di-σ, and μ complexes $C_xH_yAu_n$ were considered; the optimized structures of the $C_2H_2Au_{12}$ and $C_2H_4Au_{12}$ complexes are shown in Fig. 2.

The stability of the Au_n cluster was evaluated from the difference between the total energies of the 3D and

2D isomers (E_{3D-2D}), the binding energies per atom in the cluster (E_b), and the energy difference between the lowest unoccupied molecular orbital (LUMO) and the highest occupied molecular orbital (HOMO) (E_g)
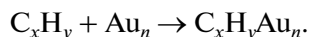
$$E_{3D-2D} = E(Au_n(3D)) - E(Au_n(2D)),$$
$$E_b = (nE(Au) - E(Au_n))/n,$$
$$E_g = E(LUMO) - E(HOMO),$$

where $E(Au)$ is the energy of the gold atom in the gas phase and $E(Au_n)$ is the total energy of the Au_n cluster.

To assess the possibility of formation of $C_xH_yAu_n$ for each cluster and type of complex, we calculated the changes in the standard Gibbs energy (ΔG_{ads}°) at 298 K in the reaction

$$C_xH_y + Au_n \rightarrow C_xH_yAu_n.$$

The differences ΔG_{ads}° were calculated from the total energies of the substance involved in the reaction ($E(C_xH_yAu_n)$, $E(C_xH_y)$, and $E(Au_n)$) and the temperature corrections ($G_{298}^\circ(C_xH_yAu_n)$, $G_{298}^\circ(C_xH_y)$, and $G_{298}^\circ(Au_n)$) calculated by the statistic thermodynamic method [26]:

$$\Delta G_{ads}^\circ = E(C_xH_yAu_n) - E(C_xH_y) - E(Au_n)$$
$$+ G_{298}^\circ(C_xH_yAu_n) - G_{298}^\circ(C_xH_y) - G_{298}^\circ(Au_n).$$

The degree of hydrocarbon activation was evaluated from the change in the C−C bond length (ΔR) in the $C_xH_yAu_n$ complex relative to the corresponding bond length in the isolated C_2H_4 (1.34 Å) and C_2H_2 (1.21 Å) molecules. The selectivity in the adsorption of acetylene compared to that of ethylene for the most stable complexes was evaluated by calculating the $\Delta G_{ads}^\circ(C_2H_2)/\Delta G_{ads}^\circ(C_2H_4)$ ratios. At $\Delta G_{ads}^\circ(C_2H_2)/\Delta G_{ads}^\circ(C_2H_4) > 1$, the acetylene adsorption is dominant. To evaluate the energy change of the cluster in the reaction with C_xH_y in each $C_xH_yAu_n$ complex, we calculated the energy of cluster distortion (E_{dis})

$$E_{dis} = E(Au_n^*) - E(Au_n),$$

where $E(Au_n^*)$ and $E(Au_n)$ are the total energies of the cluster distorted as a result of the interaction with the hydrocarbon and of the cluster before the interaction, respectively.

RESULTS AND DISCUSSION

The energies E_{3D-2D}, E_b, and E_g for the Au_{10}, Au_{12}, and Au_{20} 2D and 3D clusters are given in Table 1. The high positive values of E_{3D-2D} and E_g obtained for the Au_{10} (2D) cluster suggest that it is stable in the 2D form, which agrees with the data of [24] about the stability of the planar structure of small gold clusters. For the Au_{12} cluster, the existence of 2D and 3D isomers, which differ but slightly in energy, was predicted earlier [23]. The structural instability of the Au_{12} cluster is

Table 1. Relative energies (E_{3D-2D}, kJ/mol), binding energies (E_{bnd}, kJ/mol), and differences in HOMO−LUMO energies (E_g, eV) for 2D and 3D Au_{10}, Au_{12}, and Au_{20} clusters

Energy	Au_{10}		Au_{12}		Au_{20}	
	2D	3D	2D	3D	2D	3D
E_{3D-2D}	51		25		−207	
E_{bnd}	198	193	205	203	216	453
E_g	1.30	0.87	0.95	0.91	<0.001	1.73

confirmed by the small positive value of E_{3D-2D} and small (<1 eV) value of E_g. The stable Au_{20} isomer has a 3D structure indicated by the significant negative E_{3D-2D} and high E_g. Note that E_g increase from Au_{10} to Au_{20} because of the transition of the clusters into a more compact structure characterized by a large number of aurophilic interactions [27].

Table 2 lists the calculated ΔG_{ads}° values for interactions of the clusters with ethylene and acetylene. According to these data, ethylene can form π complexes with the Au_{10}, Au_{12}, and Au_{20} 2D and 3D isomers and di-[pi] complexes with the Au_{10} and Au_{12} 2D and 3D isomers.

The π-$C_2H_4Au_n$ complexes are formed when the hydrocarbon is coordinated to the gold atom that forms a vertex and an angle in the 3D and 2D clusters, respectively. For di-σ-$C_2H_4Au_n$, the center of adsorption is the Au(vertex)−Au(edge) fragment. A change in the C−C distance in the complexes compared with the C−C distance in C_2H_4 (ΔR, Table 2) points to a more significant activation of ethylene in the di-σ complexes ($\Delta R = 0.11 \pm 0.03$ Å) relative to that in the π complexes ($\Delta R = 0.05 \pm 0.01$ Å). A comparison of the ΔG_{ads}° values for π-$CC_2H_4Au_n$ and di-σ-$C_2H_4Au_n$ shows that the formation of the π complex is preferable for ethylene irrespective of the structure and composition of the cluster (Table 1). A similar conclusion was made in the quantum-chemical modeling of ethylene adsorption on small Au_n clusters ($n = 1-10$) [28] and structure elucidation of ethylene complexes adsorbed on the surface of gold electrodes [29].

Let us correlate the calculated ΔG_{ads}° values for the formation of π-$C_2H_4Au_n$ with the peculiarities of the structure and electronic structure of the cluster. On passing from Au_{10} to Au_{20}, ΔG_{ads}° increased (in magnitude) from −34 to −41 kJ/mol for the 2D isomers and decreased from −35 to −18 kJ/mol for the 3D isomers. The interaction of ethylene with the Au_{10} (2D and 3D) and Au_{12} (2D and 3D) clusters with E_g of ≈1 eV is characterized by almost identical ΔG_{ads}° values. In contrast to this, the Au_{20} 3D isomer with high E_g shows the lowest activity in the formation of the π complex, while its 2D isomer with low E_g shows the highest activity. The established correlation between ΔG_{ads}°

Table 2. Variation of the standard Gibbs energy at 298 K (ΔG°_{ads}, kJ/mol), cluster distortion energies (E_{dis}, kJ/mol) during the interactions of C_2H_4 and C_2H_2 with the 2D and 3D Au_{10}, Au_{12}, and Au_{20} clusters, and variation of the C−C bond of the hydrocarbon during the formation of the $C_xH_yAu_n$ complex (ΔR, Å)

Cluster		π type			di-σ type		
		$-\Delta G^\circ_{ads}$	E_{dis}	ΔR	$-\Delta G^\circ_{ads}$	E_{dis}	ΔR
		$C_xH_y = C_2H_4$					
Au_{10}	2D	34	5	0.05	10	6	0.10
	3D	35	11	0.06	6	33	0.13
Au_{12}	2D	32	5	0.05	9	12	0.08
	3D	34	9	0.06	26	9	0.09
Au_{20}	2D	41	5	0.05	14	15	0.14
	3D	18	5	0.04	−	−	−
		$C_xH_y = C_2H_2$					
Au_{10}	2D	32	5	0.02	36	6	0.09
	3D*	38	11	0.04	28	33	0.15
Au_{12}	2D	31	5	0.04	13	12	0.08
	3D**	32	9	0.04	51	9	0.09
Au_{20}	2D	68	2	0.03	51	9	0.10
	3D	18	5	0.03	−24	12	0.08

* Formation of the μ complex: $\Delta G^\circ_{ads} = -37$ kJ/mol, $E_{dis} = 88$ kJ/mol, and $\Delta R = 0.16$ Å.

** Formation of the μ complex: $\Delta G^\circ_{ads} = -78$ kJ/mol, $E_{dis} = 69$ kJ/mol, and $\Delta R = 0.17$ Å.

and E_g is determined by the mechanism of the formation of the π complex on the surface of transition metals. As is known, the C−C bond of olefin interacts with the gold atom according to the donor–acceptor mechanism [28]. The energy of the π complex decreases during the overlap of the binding orbitals of gold and olefin, thus increasing the adsorption energy. The structure of the cluster changes slightly during the formation of π-$C_2H_4Au_n$. The calculated E_{dis} values are small (5–11 kJ/mol). In contrast to π-$C_2H_4Au_n$, the possibility that di-σ-$C_2H_4Au_n$ will form depends strongly on the cluster distortion energy. The structurally rigid Au_{10} (3D) with high E_{dis} has the lowest ΔG°_{ads} (−6 kJ/mol). In contrast, the "dynamic" Au_{12} (3D) shows high activity in the formation of the di-σ complex ($\Delta G^\circ_{ads} = -26$ kJ/mol).

Acetylene can form π complexes with the Au_{10}, Au_{12}, and Au_{20} 3D and 2D isomers, di-σ complexes with the Au_{10} and Au_{12} 3D and 2D isomers, and μ complexes with Au_{10} (3D) and Au_{12} (3D). As in the case of ethylene, the π-$C_2H_2Au_n$ complexes form by hydrocarbon coordination to the gold atom, which forms a vertex of the 3D cluster or an angle of the 2D cluster. For di-σ-$C_2H_2Au_n$, the Au(vertex)−Au(edge) fragment is the adsorption center. The formation of μ-$C_2H_2Au_n$ demands the presence of special Au_3 structural fragments (Fig. 1f), which are present in Au_{10} (3D) and Au_{12} (3D). The

π-$C_2H_2Au_n$, di-σ-$C_2H_2Au_n$, and μ-$C_2H_2Au_n$ complexes differ in the degree of activation of acetylene; the C−C bond is maximally extended in μ-$C_2H_2Au_n$ (3D). For μ-$C_2H_2Au_n$, ΔG°_{ads} is −37 and −78 kJ/mol for Au_{10} (3D) and Au_{12} (3D), respectively. The stability of the μ complexes can be explained in terms of the degree of the reverse shift of electron density from the hydrocarbon to the unoccupied orbitals of gold in the adsorbed complexes. Thus the reverse shift is only 20% in the di-σ complex, very insignificant in the π complex, and approximately 50% in the μ complex [30].

Let us correlate the calculated ΔG°_{ads} values for the formation of the π, di-σ, and μ-$C_2H_4Au_n$ complexes with the peculiarities of the structure and electronic structure of the cluster. For acetylene bound according to the π and di-σ types, the tendencies are the same as for ethylene (Table 2), namely, for π-$C_2H_2Au_n$, ΔG°_{ads} increases (in magnitude) from −32 to −68 kJ/mol on passing from Au_{10} to Au_{20} for the 2D isomers and decreases from −38 to −18 kJ/mol for the 3D isomers. Also, there is an inverse relationship between ΔG°_{ads} of π-$C_2H_2Au_n$ and E_g of the cluster. As in the case of ethylene, ΔG°_{ads} for di-σ-$C_2H_2Au_n$ are related to the distortion energy of the cluster. Because of the positive ΔG°_{ads} (+24 kJ/mol), the stable Au_{20} (3D) cluster cannot form di-σ complexes with acetylene. In contrast,
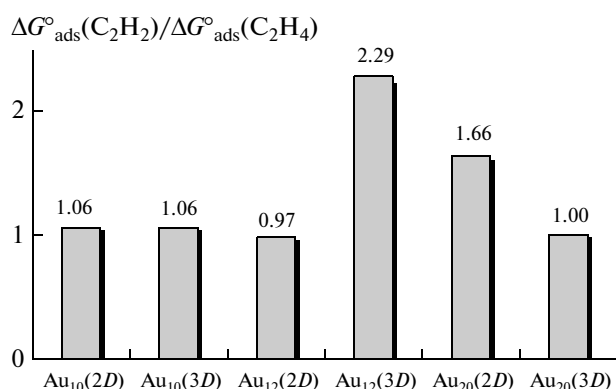
$\Delta G°_{ads}(C_2H_2)/\Delta G°_{ads}(C_2H_4)$

Fig. 3. Selectivity of adsorption of acetylene relative to that of ethylene ($\Delta G^{\circ}_{ads}(C_2H_2)/\Delta G^{\circ}_{ads}(C_2H_4)$) on gold clusters.

the Au_{12} (3D) cluster shows high activity during acetylene coordination according to the di-σ type. The formation of the μ complex is favored by the dynamic structure of the Au_{12} (3D) cluster and the presence of special structural Au_3 fragments in Au_{10} (3D) and Au_{12} (3D).

As mentioned above, hydrogenation occurs selectively if adsorption of acetylene is stronger than that of ethylene [8]. Figure 3 shows the variation of the calculated adsorption selectivities $\Delta G^{\circ}_{ads}(C_2H_2)/\Delta G^{\circ}_{ads}(C_2H_4)$ depending on the type of the cluster. The Au_{12} (3D) and Au_{20} (2D) clusters have the highest $\Delta G^{\circ}_{ads}(C_2H_2)/\Delta G^{\circ}_{ads}(C_2H_4)$ value and hence facilitate the selective adsorption of acetylene.

The considerable activation of acetylene on Au_{12} (3D) is related to the formation of the μ complex. The formation of such complexes is favored by the presence of special trigonal Au_3 fragments in gold nanoparticles. The concentration of Au_3 fragments is proportional to the number of atoms that form the edges of the model clusters (Fig. 1f). The high selectivity in acetylene adsorption on Au_{20} (2D) is due to the large ΔG°_{ads} value for the π-$C_2H_2Au_n$ complex, whose formation involves the angular gold atoms with a low coordination number. Thus the selectivity of hydrogenation in real catalysts should be determined by the number of atoms with an uncrowded coordination sphere and located on the edges and at the vertices of nanoparticles.

As is known, the number of edge and angular fragments in real particles increases when the particle size decreases [1, 2]; therefore, high selectivity of hydrogenation should be expected for small gold particles. This assumption is consistent with the results of [6, 31]. It was shown [31] that the selectivity increased 20-fold when the gold particle size decreased from 8 to 2.5 nm. The number of atoms with an unsaturated coordination sphere can be increased by doping gold with the oxide of another metal. This was done in the case of highly selective Au−NiO catalysts of acetylene hydrogenation into ethylene [10].

CONCLUSIONS

Thus the interaction of ethylene with 2D and 3D Au_{10}, Au_{12}, and Au_{20} clusters can form π and di-σ complexes. The ethylene π complexes form if the clusters contain angular atoms with low coordination numbers and low HOMO−LUMO energy differences. The di-σ complexes form if the cluster contains edge elements. The degree of ethylene activation in di-σ-$C_2H_4Au_n$ is higher than that in π-$C_2H_4Au_n$. Acetylene forms π, di-σ, and μ complexes depending on the properties of the surface. The vertices of the cluster are the centers of π type coordination of acetylene and the edges are the centers of di-σ coordination. The dynamic structure of the surface and the presence of special Au_3 structural fragments favor the formation of the μ complex. The highest activation of acetylene was observed in the μ complex. Selective adsorption of acetylene relative to ethylene is possible on the Au_{12} (3D) and Au_{20} (2D) clusters. The formation of a catalyst from gold particles having Au_{12} (3D) and Au_{20} (2D) structural units should increase the selectivity of acetylene hydrogenation to ethylene.

REFERENCES

1. A. S. K. Hashmi and G. J. Hutchings, Angew. Chem., Int. Ed. Engl. **45**, 7896 (2006).
2. V. I. Bukhtiyarov, Russ. Chem. Rev. **76**, 553 (2007).
3. M. A. Keane, S. Gómez-Quero, and F. Cárdenas-Lizana, Chem. Catal. Chem. **1**, 270 (2009).
4. V. V. Smirnov, S. A. Nikolaev, G. P. Murav'eva, et al., Kinet. Catal. **48**, 265 (2007).
5. L. McEwan, M. Julius, S. Roberts, et al., Gold Bull. **43**, 298 (2010).
6. J. Jia, K. Haraki, J. N. Kondo, K. Domen, et al., J. Phys. Chem. B **104**, 11153 (2000).
7. S. A. Nikolaev, L. N. Zanaveskin, V. V. Smirnov, et al., Russ. Chem. Rev. **78**, 231 (2009).
8. A. Molnár, A. Sárkány, and M. Varga, J. Mol. Catal. A **173**, 185 (2001).
9. A. Fahmi and R. A. van Santen, Surf. Sci. **371**, 53 (1997).

10. S. Nikolaev, D. Pichugina, and D. F. Mukhamedzyanova, Gold Bull. **45**, 221 (2012).

11. E. Bus, D. E. Ramaker, and J. A. van Bokhoven, J. Am. Chem. Soc. **129**, 8094 (2007).

12. G. A. Somorjai and J. Y. Park, Angew. Chem., Int. Ed. Engl. **47**, 9212 (2008).

13. B. Hammer, Y. Morikawa, and J. K. Norskov, Phys. Rev. Lett. **76**, 2141 (1996).

14. S. N. Lanin, Yu. G. Polynskaya, D. A. Pichugina, et al., Russ. J. Phys. Chem. A **87**, 1520 (2013).

15. D. A. Pichugina, S. N. Lanin, A. V. Beletskaya, et al., Russ. J. Phys. Chem. A **86**, 1892 (2012).

16. Z. W. Wang and R. E. Palmer, Nanoscale **4**, 4947 (2012).

17. S. N. Lanin, D. A. Pichugina, A. F. Shestakov, et al., Russ. J. Phys. Chem. A **84**, 2133 (2010).

18. Jun Li, Xi Li, Hua-Jin Zhail, and Lai-Sheng Wang, Science **299**, 864 (2003).

19. *Catalysis: Principles, Types and Applications*, Ed. by Minsuh Song (Nova Science, New York, 2011), p. 245.

20. J. P. Perdew, K. Burke, and M. Ernzerhof, Phys. Rev. Lett. **77**, 3865 (1996).

21. K. G. Dyall, J. Chem. Phys. **100**, 2118 (1994).

22. D. N. Laikov, *PRIRODA*, Electronic Structure Code, Vers. 6 (2006).

23. D. F. Mukhamedzyanova, N. K. Ratmanova, D. A. Pichugina, et al., J. Phys. Chem. C **116**, 11507 (2012).

24. Li Xiao, Bethany Tollberg, Xiankui Hu, and Lichang Wang, J. Chem. Phys. **124**, 114309 (2006).

25. E. S. Kryachko and F. Remacle, Int. J. Quantum Chem. **107**, 2922 (2007).

26. V. D. Yagodovskii, *Statistical Physics* (BINOM, Labor. Znanii, Moscow, 2005) [in Russian].

27. Xi-Bo Li, Hong-Yan Wang, Xiang-Dong Yang, et al., J. Chem. Phys. **126**, 084505 (2007).

28. A. Lyalin and T. Taketsugu, J. Phys. Chem. C **114**, 2484 (2010).

29. M. L. Patterson and M. J. Weaver, J. Phys. Chem. **89**, 1331 (1985).

30. E. Bus, R. Prins, and J. A. van Bokhoven, Catal. Commun. **8**, 1397 (2007).

31. S. Nikolaev and V. V. Smirnov, Gold Bull. **42**, 182 (2009).

Translated by L. Smolina

SPELL: OK